In Vivo Imaging of Small Animals using Radioisotopes and Position-Sensitive Photomultipliers

A thesis submitted in partial fulfillment of the requirements for the degree of Bachelor of Science in Physics from the College of William and Mary in Virginia,

by

William Thomas Hammond

Williamsburg, Virginia
May 9, 2005

Acknowledgements

In the following pages, I describe a research project that was made possible by the collaborative effort of scientists from the Physics, Biology, and Applied Science departments at William & Mary, as well as by members of the detector group at the Jefferson National Accelerator Facility. As the most recent addition to the list of collaborators, I have several individuals to thank for their academic and personal guidance over the past two semesters. My advisor, Dr. Robert Welsh of Physics, bestowed upon me incalculable guidance. I will forever be grateful for his tutoring, mentoring, and support on both academic and career issues. Also, the interdisciplinary nature of this research allowed me to benefit from the guidance of two additional professors - both from the Biology department. Dr. Eric Bradley's ability and willingness to clearly explain the biological intricacies of our research helped me immensely. Dr. Margaret Saha's kind support and tutoring greatly enhanced my scientific writing ability. I truly felt privileged to benefit from the focused guidance of three such personable, generous, and knowledgeable individuals. Finally, I would like to thank Applied Science graduate student Jianguo Qian for his generous technical support and enlightenment.

My role in this research was supported in part by a Howard Hughes Medical Institute grant through the Undergraduate Biological Sciences Education Program to the College of William & Mary.

Abstract

For decades, scientists have recommended potassium iodide (KI) to block human thyroid uptake of radioactive iodine in the event of nuclear breach of containment. Numerous studies have examined thyroid activity 24 hours or longer after initial exposure to radioiodine. These studies determined effective KI dosage levels for humans. This study examined the dynamic bio-distribution of ^{125}I continuously during the first hour after exposure in mice using a position-sensitive planar gamma camera. Various dosages of potassium iodide were systematically tested to determine the most effective blocking dose for mice. The results showed that the human recommended dose, when scaled to the mass of a mouse, does not completely block thyroid uptake of radioiodine. Compared to unblocked mice one hour after exposure to radioactive iodine, the single scaled human dose only blocked 48% of the radioiodine. However, five times the human-recommended dose (scaled to a mouse) blocked 71% of the uptake.

Table of Contents

List of Figures

List of Tables

1 Introduction

Exposure to various isotopes of iodine has been a health concern for many years due to its widespread presence in modern technologies. Radioactive iodine, especially ^{131}I and ^{125}I, is incorporated effectively into many radiopharmaceuticals. A wide range of human medicinal methods use iodine radiotracers. One example is ^{131}I radiotherapy of patients with Graves' disease. Radiotracers are also heavily used in rodent and human medical research. Furthermore, nuclear fission reactions result in a large excess of radioiodine waste products. The most significant products are ^{131}I and ^{129}I, as they are the only fission-produced isotopes of iodine with half-lives greater than one day [1]. All uses of and exposure to radioactive iodine produce a single unifying concern: potentially adverse health effects on the thyroid.

The presence of inorganic iodine in the diet is essential for proper thyroid function. The mammalian thyroid needs inorganic iodine to synthesize the hormones thyroxine (T3) and triiodothyronine (T4). To this end, the sodium iodide (Na^+/I^-) symporter (NIS), an integral membrane protein expressed in thyroid epithelial cells, facilitates the diffusion of free iodine from the blood into the thyroid. Iodine is accumulated and stored in the thyroid for organification into T3 and T4 [2]. Radioactive iodine poses an especially dangerous health risk to the thyroid because the (NIS) does not differentiate between isotopes of iodine. Thus, thyroid exposure to radioiodine results in uptake and organification of radioactive iodine, prolonging exposure to gamma-ray and X-ray decay. The high thyroid radiation doses resulting from radioiodine exposure have been shown to greatly increase thyroid cancer rates. The increased risk of thyroid cancer due to radioiodine exposure is especially threatening to children. Thyroid cancer rates in

children near Chernobyl dramatically increased within a few years after the accident [3]. However, because the thyroid can be saturated with stable iodine, prophylactic administration of iodine prior to exposure can effectively guard against thyroidal uptake of radioactive iodine. The most widely accepted form of stable iodine used for this purpose is potassium iodide (KI).

Since the breach of containment at Chernobyl, there has been significant study to determine how best to protect human thyroids from potential radioactive iodine exposure. This has always been a concern for citizens living in proximity to nuclear reactors, but the more recent threat of bioterrorism has increased overall concern. Due to this concern, several studies have tested the effectiveness of stable iodine (usually potassium iodide) under various conditions in blocking thyroidal uptake of radioiodine in humans. The following section briefly describes the findings of some of these studies.

2 Literature Review

The ability of potassium iodide to block thyroidal uptake of radioactive iodine has been well studied in the past, mostly encouraged by nuclear safety concerns. To determine a dosage to be used for protection of human thyroids in the event of an emergency, a few studies were done from the late 1960s into the early 1980s.

Blum and Eisenbud tested the effect of administered KI on radioiodine uptake in thyroids of euthyroid adults [4]. This study proclaimed that administration of 100 to 200 mg of potassium iodide (78 to 153 mg pure iodine) blocked uptake by 98%. However, the data in this study vary significantly, with the standard deviation of the control group equaling 33% of the mean. Nevertheless, when looking 24 hours after radioiodine exposure, Blum and Eisenbud conclusively show that a prophylactic dose of 100 mg KI substantially lowers thyroid activity.

The effectiveness of a 100 mg dose of KI is fairly well supported in the literature [5-6]. The findings of these studies were also a result of examining the activity in the thyroid twenty-four hours or later after administration of radioactive iodine. Each used a scintillating counter placed adjacent to the neck of the patient to measure activity.

Sternthal et al, however, concluded that less iodide was needed to protect the human thyroid [7]. According to this study, a dose as small as 30 mg sodium iodide (25 mg pure iodine) can reduce the twenty-four hour activity by more than 90%. Higher doses are shown to provide indiscernible advantage. The findings of Sternthal et al are important, because in large-scale prophylaxis, the lowest dose with the maximum effect is desired. Overdose of KI can cause moderate to severe side effects in humans,

including iodine-induced goiter and even death in some individuals sufficiently allergic [8].

Most previous studies looked at thyroid activity at least 24 hours after exposure. Although 100 mg KI is shown to result in a well-protected thyroid 24 hours after exposure, little evidence exists in the literature to conclude this dosage sufficiently protects immediately after exposure.

One study has applied potassium iodide blocking to a mouse model. Zuckier et al administered 60 μg super-saturated KI to mice and used a whole-body scintillation counter to measure radioiodine retention 24, 48, and 72 hours after exposure [9]. They found that, when compared to control mice, 15% radioiodine was still present in the body of blocked animals after 24 hours.

3 Purpose

The purpose of this study was to systematically determine the most effective potassium iodide thyroid-blocking dose for mice. Once determined, this dosage can be used in thyroid-blocking protocols for mouse-model medical studies using iodine radiotracers. In such studies, it can be beneficial to block thyroid uptake of radioiodine in order to focus on other regions of interest. While previous studies have looked at radioiodine retention 24 hours after exposure, this study looks at thyroid activity immediately following exposure.

Time of measurement is critical in many biochemical medical studies. Metabolism of radiotracers, like iodine, can be extremely rapid. In mouse-model studies investigating biodistributions of radiotracers, it is important to effectively block immediately following radiotracer injection. Therefore, this study looked at the distribution of radioiodine from 0-60 minutes after exposure to determine KI blockade effectiveness in the first hour after exposure.

When counting decay 24 hours or more after administration of radioactive iodine, as was done in most previous studies, there is little background radiation to interfere with measurement of the thyroid. Thus, it was acceptable to simply place a Geiger or crystal scintillation counter next to the neck of the (human) subject to measure the activity of the thyroid. However, when imaging closer to the time of radiotracer administration or when imaging regions of small size, high precision of detection locality is essential. Thus, this study employed high precision position-sensitive detection.

4 Materials and Methods

4.1 Gamma camera

This study employed a fixed, two-dimensional gamma camera to examine the rapid distribution of radioiodine in the body of a mouse [10-14]. The apparatus consisted of a 5 inch diameter Hamamatsu R3292 position-sensitive photomultiplier tube (PSPMT) coupled with an array of CsI(Tl) scintillating crystals and a parallel-hole collimator (FIG. 1). As shown in the picture, the gamma camera is secured to a rotating gantry for use in Single Photon Emission Computed Tomography (SPECT) imaging. This type of imaging allows a three-dimensional image to be reconstructed from multiple two-dimensional "slices" generated by slowly rotating a gamma camera around the source being imaged. Because the metabolism of radioiodine in mice is initially extremely rapid, three-dimensional reconstruction of mice in the first hour after exposure to ^{125}I is not possible. Therefore, in these studies, the gantry remains fixed, producing planar imaging.

The face of the R3292-02 PSPMT was air coupled to a CsI(Tl) scintillating crystal array (manufactured by Hilger Analytical Ltd.). The pixellated scintillator array was composed of 1 x 1 x 3 mm pixels with a crystal element pitch of 1.25 mm. This size crystal works well with ^{125}I, as most of the emitted 35 keV photons are stopped within the first 1 mm of CsI(Tl). Thus, efficient conversion is achieved into the spectral response range of the R3292-02 (300 – 650 nm). The crystal elements were separated by a thick diffuse white reflecting glue that also covers the backside of the array. Finally, a parallel-hole collimator was secured directly on top of the crystal array in order to limit the field

of view of any single crystal. The collimator ensures that the photons to be detected are roughly perpendicularly incident upon the crystals.

The Hamamatsu R3292-02 PSPMT has 28x28 crossed anode output wires. By connecting anode wires in sector groups of two, the number of channels to amplify and digitize was reduced by a factor of two. These 14x14 remaining output grouped wires were fed through a Computer Automated Monitor and Control, Fast Encoding and Readout, Analog to Digital Converter (CAMAC FERA ADC) for digitization.

The imaging system used in this study has general advantages over alternative approaches. *In vivo* imaging does not require subject sacrifice. The animals serve as their own controls during longitudinal studies. Furthermore, the use of a position-sensitive gamma camera provides the opportunity for continuous and simultaneous evaluation of all body portions over time.

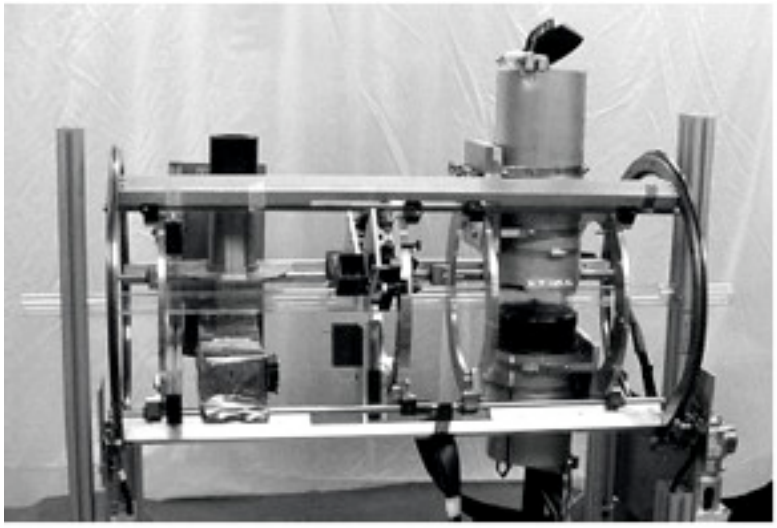

FIGURE 1. Two gamma cameras are fixed on the right side of the gantry facing each other (mounted vertically). The gamma cameras consist of a PSPMT coupled with a planar array of scintillating crystals and parallel-hole collimators.

4.2 KI Dosage and Mouse Imaging

Based on the findings of previous studies (described in the Literature Review section) the FDA and World Health Organization (WHO) currently recommend administration to human adults of 130 mg potassium iodide prior to exposure to radioiodine [15-16]. The FDA scales this dose down to 65 mg for children and adolescents between the ages of 3 and 18, 32 mg for toddlers, and 16 mg for infants. For this study, the adult dosage of 130 mg was scaled down to a corresponding mass-dependent dose (1.85 μg/mg) for mice (this is referred to as the scaled human dose). Higher dosages were tested, including 5.55 μg/mg (3X scaled human dose), 9.25 μg/mg (5X scaled human dose), and 18.5 μg/mg (10X scaled human dose).

Twenty mice were imaged with the gamma camera for this study. In non-control animals, one of five mass-dependent KI dosages was orally administered one hour prior to imaging. After administering KI, animals were held in cages for fifty-five minutes. Five minutes prior to imaging, the animals were administered dilute sodium pentobarbital. Immediately following anesthetization, radioactive iodine ($Na^{125}I$), was introduced into the body of the mouse through an intramuscular injection into the femoral biceps of the right leg. The target dose level for each mouse was approximately 14 μCi; the actual administered doses varied slightly from this target, and were recorded. Finally, the mouse was placed directly onto the gamma camera. The mice were imaged for a total of one hour, and then returned to their cages.

4.3 Data collection

The data output of the gamma camera was interpreted by a sophisticated collection of computer equipment and programming. The CAMAC FERA ADC digitized output was fed into a Mac G3 running KMAX software (Sparrow, Inc.). KMAX recorded each photon detected by the gamma camera as an "event." Each event included the time, energy, and position of detection. KMAX associates each of these events with one of 4096 positions (pixels) in the plane of the detector. These event-file data were fed into a Mac G4 for further processing using analysis programs written in the data processing and visualization language IDL (Research Systems, Inc.).

First, IDL was used to group event-files into five-minute time intervals, creating twelve grouped, time-dependent event-files. Each of these files held a "snapshot" image that associated each position in the plane of the mouse with the number of photons detected (originating from that position) over the five-minute time interval. Thus, when imaging a mouse for one-hour, twelve files were created. Each file encoded the number of recorded events summed over five-minute time intervals in each of 4096 positions. With this simplified grouping of event files, another IDL-based program was used to choose any region in the plane over which to sum position-sensitive detected signals. This program permits time-dependent detection analysis of any chosen region, for instance the localized thyroid region. Thus, using these analysis methods, it was possible to observe and compare a quantified distribution of ^{125}I over various selected physiological regions within the body of a mouse continuously in time.

4.4 Data analysis

The goal of these analyses was to calculate the concentration of radioiodine only within the thyroid, not the surrounding tissue. Using planar gamma ray imaging, one cannot see the internal physiology of a mouse. Instead, isolated decay regions give clues as to where specific physiological regions lie. For this study, estimates are valid because the thyroid provides an isolated region of concentrated decay, making it relatively easy to isolate and analyze. However, planar gamma imaging is unable to isolate tissues of interest in the dimension perpendicular to the detector. Thus, planar gamma imaging inherently allows detection of radiation originating from tissues (and/or blood content) extraneous to the tissue of interest. Therefore, the general thyroid region, when saturated with radioactive iodine, emits two radiation types: thyroid activity and non-thyroid activity (tissue which locally surrounds the thyroid).

Two forms of non-thyroid activity challenged precision of thyroid uptake measurements. First, the sub-maxillary glands express the NIS, and therefore absorb a higher than average dose of radiation. Because the sub-maxillaries are situated adjacently to the thyroid, it was necessary to ensure that measurements were not skewed by their presence. Two regions of interest were selected for analysis of radioiodine uptake: the first was a small region within the boundaries of the thyroid itself, while the second was a larger region that encompassed both the thyroid and sub-maxillaries. Differences and similarities between the radioiodine distributions in these two regions were analyzed to determine the effect, if any, of the submaxillary glands on measurements of the thyroid.

Furthermore, because mice were imaged in the first hour after exposure to radioiodine, a large portion of the total radiation dose administered remained in the blood stream during imaging. Therefore, part of the detected activity of the thyroid region was due to blood content of the thyroid and surrounding vascularized tissue. A model was generated to correct for this general vascular bed activity. The leg region does not contain any tissue known to actively accumulate iodine, and also showed the most consistent (though very low) uptake throughout all treatments. Therefore, it served as a suitable tissue to estimate the vascular bed radioactivity.

Three physiological regions were analyzed to create useful comparisons: the thyroid region(s), the leg, and the body as a whole. For each of these regions, decays were counted and summed into twelve five-minute groups (see Materials and Methods, Data collection). The left leg (the radiation dose was injected into the right leg) modeled the non-facilitated diffusion of iodine into tissue and the iodine concentration of local blood flow. The physical area over which decays were counted in the thyroid was not equal to that of the leg. Therefore, leg counts were scaled to reflect the number of counts that would arise from a comparable leg region of an area equal to that of the thyroid region (different scaling for small and large thyroid regions). These scaled leg counts were subtracted from the thyroid counts, generating a measurement of the decay events originating from the thyroid without counting the surrounding tissue. Because mice received slightly varying total radiation doses, absolute values for decay originating in the thyroid are not translatable between trials. Therefore, leg-normalized uptake in the thyroid was compared with the total body radioactivity and expressed as an uptake ratio.

5 Summary of Results

Data were taken for twenty mice divided among the following five groups: control 0X (n=4), 1X (n=4), 3X (n=5), 5X (n=4), and 10X (n=3) the human KI blocking dose (as described above). For each mouse, two methods of analysis were employed to compare thyroidal uptake of radioiodine to injected dose. Both methods showed marked decline in thyroid uptake with increased administered dosage of potassium iodide. All blocking doses (1X, 3X, 5X, 10X) showed a decline in radioiodine uptake by the thyroid. Focusing on the radiation detected from 55-60 minutes after exposure, uptake appeared to fall off approximately exponentially with increasing KI dosage. Although 1X KI (human dose) decreased uptake significantly, higher doses clearly were more effective in blocking the thyroid in the first hour after exposure. Administration of 5X dosage or higher provided the best protection against radioiodine. The 3X dose provided intermediate protection between the 1X and 5X (and 10X) doses. Graphs of the average decay ratios across each dosage group, detected 55-60 minutes after exposure, appear in FIG. 3 & FIG. 4.

6 Data

TABLE I. Thyroid uptake ratio calculated by both small and large thyroid region analyses of control animals over the course of one hour of imaging.

Time period	Mean Ratio (small)[a]	σ (small)[b]	Mean Ratio (large)[c]	σ (large)[d]
0-5	0.0093	0.0034	0.0391	0.0136
5-10	0.0140	0.0034	0.0563	0.0172
10-15	0.0181	0.0033	0.0718	0.0137
15-20	0.0197	0.0032	0.0805	0.0124
20-25	0.0217	0.0037	0.0834	0.0147
25-30	0.0223	0.0027	0.0914	0.0099
30-35	0.0229	0.0022	0.0925	0.0107
35-40	0.0258	0.0011	0.1011	0.0037
40-45	0.0248	0.0016	0.1027	0.0052
45-50	0.0259	0.0017	0.1002	0.0087
50-55	0.0282	0.0012	0.1079	0.0072
55-60	0.0284	0.0015	0.1082	0.0062

[a]mean uptake ratio (by small thyroid analysis) of 4 animals imaged in control group
[b]standard deviation of small thyroid analysis mean thyroid uptake ratio
[c]mean uptake ratio (by large thyroid analysis) of 4 animals imaged in control group
[d]standard deviation of large thyroid analysis mean thyroid uptake ratio

TABLE II. Thyroid uptake ratio calculated by both small and large thyroid region analyses of 1X KI animals[a] over the course of one hour of imaging.

Time Period	Mean Ratio (Small)[b]	σ (Small)[c]	Mean Ratio (Large)[d]	σ (Large)[e]
0-5	0.0057	0.0020	0.0222	0.0124
5-10	0.0092	0.0017	0.0410	0.0073
10-15	0.0117	0.0015	0.0513	0.0023
15-20	0.0109	0.0012	0.0541	0.0016
20-25	0.0148	0.0020	0.0607	0.0032
25-30	0.0136	0.0018	0.0603	0.0032
30-35	0.0139	0.0024	0.0604	0.0036
35-40	0.0138	0.0018	0.0628	0.0056
40-45	0.0140	0.0017	0.0626	0.0049
45-50	0.0137	0.0027	0.0560	0.0055
50-55	0.0156	0.0027	0.0607	0.0047
55-60	0.0147	0.0016	0.0698	0.0061

[a]1X scaled human dose (1.85 μg KI / g body mass) blocked mice
[b]mean uptake ratio (by small thyroid analysis) of 4 animals imaged in 1X dosage group
[c]standard deviation of small thyroid analysis mean thyroid uptake ratio
[d]mean uptake ratio (by large thyroid analysis) of 4 animals imaged in 1X dosage group
[e]standard deviation of large thyroid analysis mean thyroid uptake ratio

TABLE III. Thyroid uptake ratio calculated by both small and large thyroid region analyses of 3X KI animals[a] over the course of one hour of imaging.

Time period	Mean Ratio (small)[b]	σ (small)[c]	Mean Ratio (large)[d]	σ (large)[e]
0-5	0.0083	0.0011	0.0407	0.0045
5-10	0.0101	0.0012	0.0498	0.0048
10-15	0.0116	0.0017	0.0561	0.0042
15-20	0.0111	0.0016	0.0554	0.0050
20-25	0.0116	0.0019	0.0568	0.0057
25-30	0.0107	0.0016	0.0521	0.0045
30-35	0.0117	0.0014	0.0562	0.0049
35-40	0.0122	0.0016	0.0558	0.0044
40-45	0.0123	0.0013	0.0554	0.0028
45-50	0.0119	0.0015	0.0559	0.0047
50-55	0.0118	0.0016	0.0542	0.0056
55-60	0.0117	0.0015	0.0531	0.0044

[a]3X scaled human dose (5.55 μg KI / g body mass) blocked mice
[b]mean uptake ratio (by small thyroid analysis) of 5 animals imaged in 3X dosage group
[c]standard deviation of small thyroid analysis mean thyroid uptake ratio
[d]mean uptake ratio (by large thyroid analysis) of 5 animals imaged in 3X dosage group
[e]standard deviation of large thyroid analysis mean thyroid uptake ratio

TABLE IV. Thyroid uptake ratio calculated by both small and large thyroid region analyses of 5X KI animals[a] over the course of one hour of imaging.

Time period	Mean Ratio (small)[b]	σ (small)[c]	Mean Ratio (large)[d]	σ (large)[e]
0-5	0.0046	0.0024	0.0244	0.0104
5-10	0.0075	0.0012	0.0367	0.0057
10-15	0.0083	0.0014	0.0438	0.0084
15-20	0.0080	0.0011	0.0408	0.0051
20-25	0.0108	0.0019	0.0510	0.0050
25-30	0.0090	0.0001	0.0455	0.0037
30-35	0.0085	0.0010	0.0424	0.0051
35-40	0.0105	0.0015	0.0519	0.0073
40-45	0.0091	0.0013	0.0451	0.0022
45-50	0.0081	0.0003	0.0424	0.0036
50-55	0.0089	0.0003	0.0470	0.0057
55-60	0.0083	0.0017	0.0441	0.0080

[a]5X scaled human dose (9.25 μg KI / g body mass) blocked mice
[b]mean uptake ratio (by small thyroid analysis) of 4 animals imaged in 5X dosage group
[c]standard deviation of small thyroid analysis mean thyroid uptake ratio
[d]mean uptake ratio (by large thyroid analysis) of 4 animals imaged in 5X dosage group
[e]standard deviation of large thyroid analysis mean thyroid uptake ratio

TABLE V. Thyroid uptake ratio calculated by both small and large thyroid region analyses of 10X KI animals[a] over the course of one hour of imaging.

Time period	Mean Ratio (small)[b]	σ (small)[c]	Mean Ratio (large)[d]	σ (large)[e]
0-5	0.0043	0.0018	0.0236	0.0111
5-10	0.0069	0.0011	0.0357	0.0117
10-15	0.0063	0.0012	0.0401	0.0078
15-20	0.0074	0.0013	0.0435	0.0049
20-25	0.0085	0.0014	0.0458	0.0084
25-30	0.0091	0.0014	0.0469	0.0066
30-35	0.0084	0.0013	0.0472	0.0100
35-40	0.0090	0.0019	0.0479	0.0108
40-45	0.0085	0.0018	0.0484	0.0100
45-50	0.0086	0.0018	0.0443	0.0100
50-55	0.0066	0.0012	0.0430	0.0102
55-60	0.0081	0.0016	0.0408	0.0082

[a]10x scaled human dose (18.5 μg KI / g body mass) blocked mice
[b]mean uptake ratio (by small thyroid analysis) of 3 animals imaged in 10X dosage group
[c]standard deviation of small thyroid analysis mean thyroid uptake ratio
[d]mean uptake ratio (by large thyroid analysis) of 3 animals imaged in 10X dosage group
[e]standard deviation of large thyroid analysis mean thyroid uptake ratio

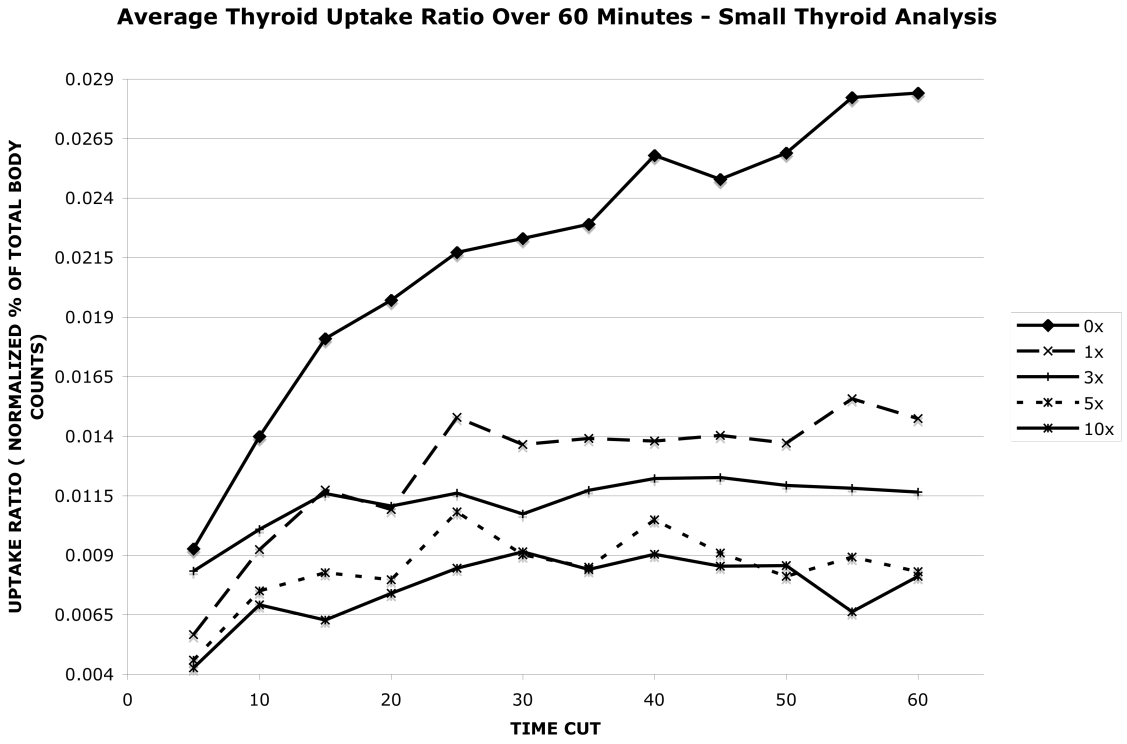

FIGURE 2. Superimposed plots comparing time of imaging to uptake ratio in the thyroid for *small* thyroid region analysis. Data points delineate average uptake (verticle axis) of all animals in blocking dose group (given by legend on right side) at the given time period (horizontal axis).

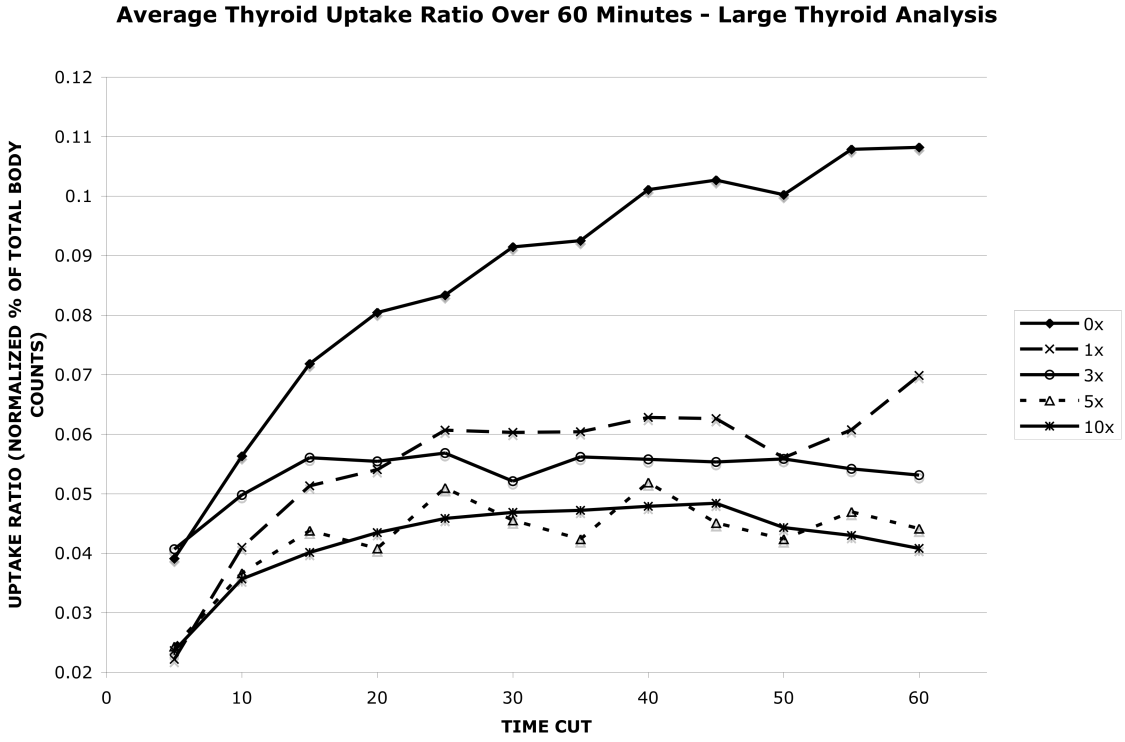

FIGURE 3. Superimposed plots comparing time of imaging to uptake ratio in the thyroid for *large* thyroid region analysis. Data points delineate average uptake (verticle axis) of all animals in blocking dose group (given by legend on right side) at the given time period (horizontal axis).

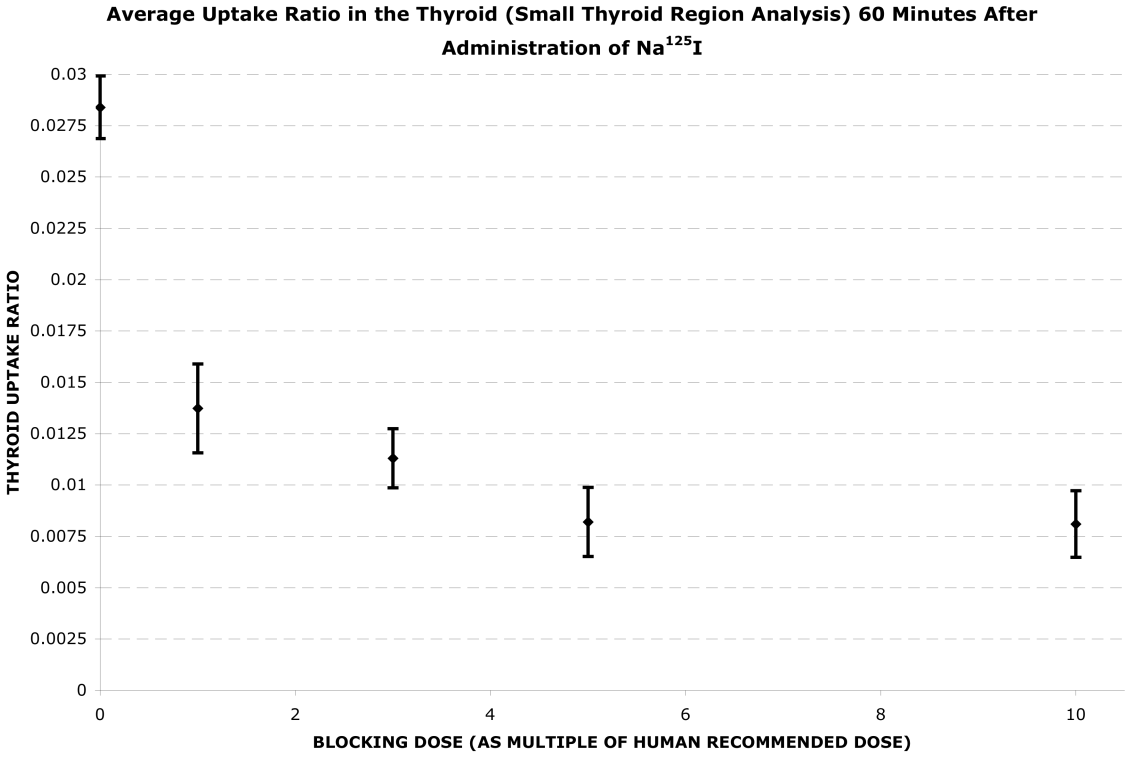

FIGURE 4. Uptake ratio in thyroid (small thyroid region analysis) after 60 minutes of imaging plotted on the vertical axis as a function of blocking dose on the horizontal axis.

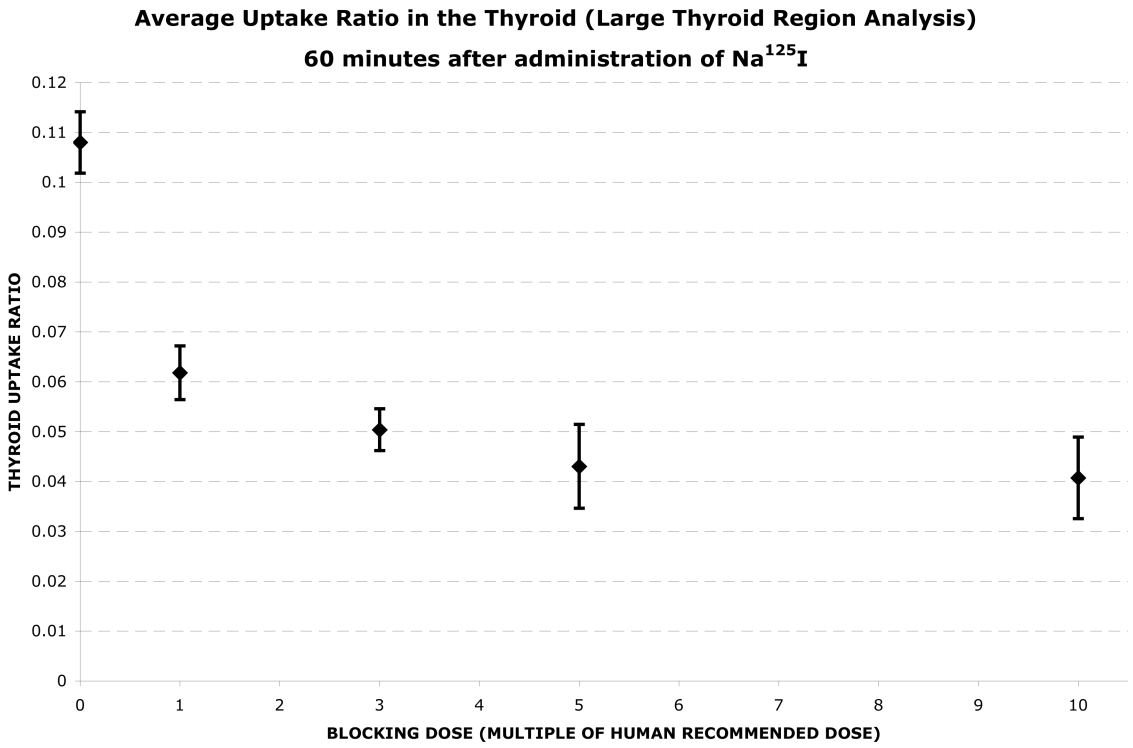

FIGURE 5. Uptake ratio in thyroid (large thyroid region analysis after 60 minutes of imaging plotted on the vertical axis as a function of blocking dose on the horizontal axis.

7 Discussion and Conclusions

During the first hour after injection into unblocked animals, radioiodine was detected throughout the body. Within the first five to ten minutes, detection showed an approximately uniform distribution throughout the body, as all vascularized tissue showed some activity. Quickly, however, the iodine began to concentrate in the thyroid, sub maxillary salivary glands, and stomach. Uptake over time in all other regions tended to reach a peak value early (~15-30 minutes), then slowly dropped over the remaining time of imaging. Thus, free diffusion of iodine through the blood and into tissue quickly reaches a saturation point. In the stomach, linear uptake was generally observed, reflecting both waste accumulation as well as NIS expression. Although stomach tissue expresses the NIS, it is not known to utilize iodine in any biological process; thus it freely exits through diffusion and does not result in prolonged exposure as in the thyroid [17]. Uptake in the thyroid, on the other hand, reflected an approximately logarithmic trend (see 0x plot in Figs. 5 & 6). This observation suggests that the rate of uptake is inversely proportional to the quantity already absorbed. The NIS continuously facilitates diffusion into thyroid cells, however, there is a saturation point at which even facilitated diffusion is no longer thermodynamically favorable.

Uptake in the thyroid of blocked mice over the first hour after exposure behaved dramatically different than that of the unblocked animal. While radioiodine concentration continuously increased in unblocked thyroid, the concentration in blocked thyroid reached a peak value early and remained approximately constant for the remainder of imaging. Each blocking dosage reduced thyroid uptake substantially; however, there were discernable differences in the degree of blocking. After one hour,

1X, 3X, 5X, and 10X potassium iodide blocked 48%, 59%, 71%, and 71%, respectively, of the detected radiation in the thyroid region, as compared to unblocked animals.

Some of the radiation in the general thyroid region of both blocked and unblocked animals originates from non-thyroid tissue. Although much of the injected radiation dose collected in the stomach, and sometimes in the urinary bladder, by the end of the hour significant quantities still remained throughout the body in vascularized tissue (none was excreted until after imaging). For this reason, the leg model for vascular bed activity was designed and implemented. However, the vascular tissue surrounding the thyroid was higher in density than in leg tissue. Therefore, the amount of radiation found in tissue surrounding the thyroid was higher than the correction factor provided by the activity of the leg. One hour after administration of radioiodine, analysis of the thyroid region still showed an average of 0.8% of total dose remaining in animals blocked with 5X and 10X potassium iodide. These low level activities found in the thyroid of 5X and 10X blocked animals are likely due to vascular and passively diffusive bed activity that was not completely subtracted from analysis of the leg region.

These data indicate that on a body mass-dependent basis, the mouse thyroid requires a more concentrated potassium iodide dosage for full protective effect. This proclamation presupposes, however, that the human recommended dose does indeed provide full thyroid protection against radioiodine uptake. These results may be of importance to small animal researchers using iodine-labeled pharmaceuticals who wish to protect the thyroid from unnecessary exposure. The results reported here suggest that small animals such as mice require substantially more KI than is currently thought necessary to protect humans.

These results may also suggest that despite the profound metabolic differences between mice and humans, there may be reason to re-evaluate the effectiveness of the human dose using more sensitive detection methods of the type used in this study. In order to relate these findings to those of previous studies, further directions include using the methods described here to measure radioiodine retention in mouse thyroid 24 hours after exposure. Furthermore, to test the potential scalability to humans of the KI dosage here determined for mice, it would first be helpful to test the scalability to a larger animal such as rat.

8 References

[1] Z. Franic, "Iodine prophylaxis and nuclear accidents." Arh hig rada toksikol **50**, 223 (1999).

[2] P. M. Conn and S. Melmed. *Endocrinology : Basic and Clinical Principles,* (Humana Press, Totowa, N.J, 1997).

[3] V. S. Kazakov, E. P. Demidchik and L. N. Astakhova, "Thyroid cancer after Chernobyl." Nature **359**, 21 (1992).

[4] M. Blum and M. Eisenbud, "Reduction of Thyroid Irradiation From ^{131}I by Potassium Iodide." JAMA. **200**, 112 (1967).

[5] K. M. Saxena, E. M. Chapman and C. V. Pryles, "Minimal Dosage of Iodide Required to Suppress Uptake of Iodine-131 by Normal Thyroid." Science **138** (1962).

[6] L. Il'in, G. Arkhangel'skaya, Y. Konstaninov and I. Likhtarev, "Radioactive iodine in the problem of radiation safety." Atomizdat (1972). (Springfield, VA: Translation series US-AEC 7536, National Technical Information Service; 1972:208-229.)

[7] E. Sternthal, L. Lipworth, B. Stanley, C. Abreau, S. Fang and L. Braverman, "Suppression of thyroid radioiodine uptake by various doses of stable iodide." N. Engl. J. Med. **303**, 1083 (1980).

[8] G. K. Macleod (Secretary of Health), Commonwealth of Pennsylvania (Harrisburg PA), "The Decision to Withhold Potassium Iodide during the Three Mile Island Event: Internal Working Document." (1979).

[9] L. S. Zuckier, Y. Li, C. J. Chang, "Evaluation in a mouse model of a thyroid-blocking protocol for ^{131}I antibody therapy." Canc. Biother. & Radiopharm. **13**, 457 (1998).

[10] J. T. Cella, "Gamma Ray Imaging of Small Animals Using Position-Sensitive Photomultiplier Tubes." Senior thesis, Department of Physics, College of William and Mary, 1-43 (2004).

[11] A. G. Weisenberger, E. Bradley, S. Majewski, and M. Saha, "Development of a Novel Radiation Imaging Detector System for in Vivo Gene Imaging in Small Animal Studies." IEEE Trans. Nucl. Sci. **145**, 1743 (1998).

[12] A. G. Weisenberger, B. Kross, S. Majewski, R. WojE. Bradley, and M. Saha, "Design Features and Performance of a CsI(Na) Array Based Gamma Camera for Small Animal Gene Research." IEEE Trans. Nucl. Sci. **145**, 3053 (1998).

[13] A. G. Weisenberger, R. Wojcik, E. L. Bradley, P. Brewer, S. Majewski, J. Qian, A. Ranck, M. S. Saha, K. Smith, M. F. Smith and R. E. Welsh, "SPECT-CT system for small animal imaging." IEEE Trans Nucl Sci. **50**, 74 (2003).

[14] M. S. Saha, E. L. Bradley, P. Brewer, K. K. Gleason, B. Kross, S. Majewski, V. Popov, J. Qian, A. Ranck, K. Smith, M. F. Smith, A. G. Weisenberger, R. Wojcik, R. E. Welsh, "Pinhole Collimators for High-resolution SPECT - Incorporation of a Fluoroscopic X-Ray Modality in a Small Animal Imaging System." IEEE Trans. Nucl. Sci. **50**, 333 (2003).

[15] US Department of Health and Human Services, Food and Drug Administration, Center for Drug Evaluation and Research, "Guidance: Potassium iodide as a thyroid blocking agent in radiation emergencies." (2001).

[16] World Health Organization (WHO), "Guidelines for iodine prophylaxis following nuclear accidents, 1999 update." (1999).

[17] N. Carrasco, "Iodide transport in the thyroid gland." BBA Rev. on Biomemb. **1154**, 65 (1993).